International Journal of Applied Power Engineering (IJAPE)
Vol. 14, No. 3, September 2025, pp. 522~532
ISSN: 2252-8792, DOI: 10.11591/ijape.v14.i3.pp522-532

Design and analysis of two switch DC-DC converters for E-vehicle applications

Jayanthi Kathiresan, Gnanavadivel Jothimani
Department of Electrical and Electronics Engineering, Mepco Schlenk Engineering College, Sivakasi, India

Article Info

Article history:

Received Feb 3, 2024
Revised Dec 27, 2024
Accepted Jan 19, 2025

Keywords:

Controller
E-vehicle
Power converter
Voltage boosting method
Voltage gain

ABSTRACT

A non-isolated DC-DC converter topology is proposed in this paper, which is distinguished by its superior performance and reduced component count in comparison to conventional converter designs. The suggested architecture is especially appropriate for applications demanding a large voltage step-up since it achieves an improved voltage conversion ratio and excellent efficiency. The addition of a voltage-boosting element, which is an inductor combined in series with a switching device, to the source side of a conventional boost converter is a unique feature of the suggested converter. To confirm the converter's operating features, a thorough theoretical analysis has been carried out, including stability and steady-state evaluations. In addition, a hardware prototype with a 200 V output and 100 W power rating was created in order to test the converter's functionality. With a peak efficiency of 94.3%, the prototype showed good agreement with analytical forecasts. The suggested converter is a viable option for renewable energy applications because of its high voltage gain, small size, and efficiency. This is especially true for solar systems and other distributed energy sources, where low component counts and high step-up ratios are preferred.

Corresponding Author:

Jayanthi Kathiresan
Department of Electrical and Electronics Engineering, Mepco Schlenk Engineering College
Sivakasi, Tamil Nadu, India
Email: kjayanthi@mepcoeng.ac.in

1. INTRODUCTION

With the increasing use of renewable power resources in industries such as automobiles and communication, switched mode power converters have become more widely used. In particular, the boost converter is commonly used in renewable power generation applications, although it does have some drawbacks, such as the reverse recovery problem of diodes. Numerous approaches for voltage boosting have been surveyed [1]. Techniques for raising voltage to reduce stress switching and increase static gain are briefly covered. In. An extensive review is presented of a non-isolated high gain converter using the voltage lift approach in [2]. A voltage raise technique boost converter with an extended topology may be found in [3]. Through experimental oversight, an efficiency of about 93.5% is obtained for a 12 V input voltage. A non-isolated step-up converter based on voltage multiplier cells has been reported in [4] for raising static voltage gain. Regenerative clamping circuitry is provided by the voltage multiplier cell in the converter, which further lessens the electromagnetic interference (EMI) issue.

The high gain DC-DC converter discussed in [5] showcases an impressive efficiency of nearly 93%. This is achieved by utilizing a clamping circuit and a voltage boost cell, alongside a coupled inductor that connects the clamping circuit and flyback converter to boost voltage gain. A double-switch converter based on complementary inverse Watkins-Johnson (CIWJ) converter is presented, which aims to increase the gain by

reducing the passive element count [6]. In [7], [8], the authors present a converter for low-power applications with fast dynamic response under load variations. The converter is designed to overcome the right half plane zero problem, which is a significant issue in conventional boost converters.

The authors inevitably addressed a coupled inductor-based converter in [9]–[11] that lowers the voltage stress on switches. The diode's reverse recovery time is a major downside of this structure. The Sheppard-Taylor converter was introduced in [12], showcasing regulated output voltage and less ripple in input and output current. This structure was designed for the non-isolated boost converter, even though the converter's voltage gain relation originally limited its operation to boost converters [13]. The importance of battery selection in electric vehicle (EV) is discussed [14]. Bidirectional resonant wireless power transfer scheme is adopted to charge the EVs is discussed in [15]. A control strategy for hybrid energy storage for speed regulation of brushless direct current (BLDC) motor is discussed [16]. In [17]-[22], authors discussed the various control schemes employed in EV for charging. The soft switching-based converter control schemes and energy management strategies employed while integrating renewable sources in EV [23]-[25].

Despite the numerous studies available power converter topology for static gain improvement and reduction in voltage drop and losses, there is still a lot of scope for research in this area. Based on the studies, a boost converter structure has been designed with a minimum number of circuit elements. Comparing the designed boost converter to the boost converter shows that the voltage boosting element consisting of an inductor and a switch improves the static voltage gain.

In this paper, the construction and operation of the modified boost converter is explained in section 1, followed by an investigation of the converter in section 2. Section 3 elaborates on the design procedure of parameters and stability study of the converter is elaborated in section 4. Section 5 discusses simulation results. In sections 6 and 7, performance comparison and experimental validation of the converter are presented, followed by conclusion.

2. EXPLANATION OF THE MBC CIRCUIT

The modified boost converter (MBC) circuit is depicted in Figure 1(a) and comprises of switches, S_1 and S_2, inductors, L_1 and L_2, a diode, D, and an output filter capacitor, C. This MBC is designed by placing an additional inductor and switching in the existing boost converter. The switches, S_1 and S_2, operate at a frequency (f_s). Certain presumptions are established to investigate the MBC's stable state of operation. First, it is assumed that semiconductor elements are ideal, and the impact of the power switches' parasitic resistance, voltage drop across the diode, analogous resistance of the inductor, and capacitors are ignored. Second, the value of inductors L_1 and L_2 is assumed to be alike. Finally, the filter capacitor C is deemed to be sufficiently huge to maintain the load voltage for the assumed load power. The MBC operates in two distinct modes, each characterized by unique V and I waveforms of the circuit elements.

2.1. Mode 1 ($t_0<t<t_1$)

In this mode, S_1 and S_2 are in conduction state, and L_1 and L_2 are energized in parallel with the voltage of V_{in}. The I_{L1} and I_{L2} inductor currents are increasing linearly with the source voltage. Diode D becomes off, and the filter capacitor C is discharged to the R_L resistor. Figure 1(b) depicts the current path direction. Using Kirchhoff's voltage law (KVL), the voltage expression of the inductors and capacitors are given in (1) to (4).

$$v_{L1} = v_{L2} = V_{in} \tag{1}$$

$$\frac{di_{L1}}{dt} = \frac{V_{in}}{L_1} \tag{2}$$

$$\frac{di_{L2}}{dt} = \frac{V_{in}}{L_2} \tag{3}$$

$$v_c = V_0 \tag{4}$$

Where v_c is the voltage across the capacitor. The state space equation of the MBC is given in (5) and (6).

$$\begin{pmatrix} \frac{di_{L1}}{dt} \\ \frac{di_{L2}}{dt} \\ \frac{dv_c}{dt} \end{pmatrix} = \begin{pmatrix} 0 & 0 & 0 \\ 0 & 0 & 0 \\ 0 & 0 & \frac{-1}{R_L C} \end{pmatrix} \begin{pmatrix} i_{L1} \\ i_{L2} \\ v_c \end{pmatrix} + \begin{pmatrix} \frac{1}{L_1} \\ \frac{1}{L_2} \\ 0 \end{pmatrix} (V_{in}) \tag{5}$$

$$V_0 = (0 \quad 0 \quad 1)\begin{pmatrix} i_{L1} \\ i_{L2} \\ v_c \end{pmatrix} \tag{6}$$

By applying Kirchhoff's current law (KCL) to Figure 1(b), the capacitor current i_c is expressed as (7) and (8).

$$i_c + i_0 = 0 \tag{7}$$

$$\frac{dv_c}{dt} = -\frac{V_0}{R_L * C} \tag{8}$$

2.2. Mode 2 (t_1<t<t_2)

During this period, switches are in off state, and L_1 and L_2 elements are in series with Vin. The diode D conducts, and the source current I_s flows through L_1, D, C, and L_2. Hence, I_{L1} and I_{L2} currents are equal to the source current I_s. Figure 2(a) illustrates the direction of the current path. The current and voltage waveforms for continuous conduction mode are illustrated in Figure 2(b). The voltage across the circuit elements by applying Kirchhoff's law. The V_{L1} and V_{L2} expressions of L_1 and L_2 are given in (9) and (10).

$$v_{L1} = \frac{V_{in} - v_c}{2} \tag{9}$$

$$v_{L2} = \frac{V_{in} - v_c}{2} \tag{10}$$

Similarly, the capacitor current I_c obtained by using KCL is given as (11) and (12).

$$I_c + I_o = I_{L1} \tag{11}$$

$$\frac{dv_c}{dt} = \frac{I_{L1}}{C} - \frac{v_c}{R_L * C} \tag{12}$$

The state space equations in matrix form are given in (13) and (14).

$$\begin{pmatrix} \frac{di_{L1}}{dt} \\ \frac{di_{L2}}{dt} \\ \frac{dv_c}{dt} \end{pmatrix} = \begin{pmatrix} 0 & 0 & \frac{-1}{2L_1} \\ 0 & 0 & \frac{-1}{2L_2} \\ \frac{1}{C} & 0 & \frac{-1}{R_L C} \end{pmatrix} \begin{pmatrix} i_{L1} \\ i_{L2} \\ v_c \end{pmatrix} + \begin{pmatrix} \frac{1}{L_1} \\ \frac{1}{L_2} \\ 0 \end{pmatrix} (V_{in}) \tag{13}$$

$$V_0 = (0 \quad 0 \quad 1)\begin{pmatrix} i_{L1} \\ i_{L2} \\ v_c \end{pmatrix} \tag{14}$$

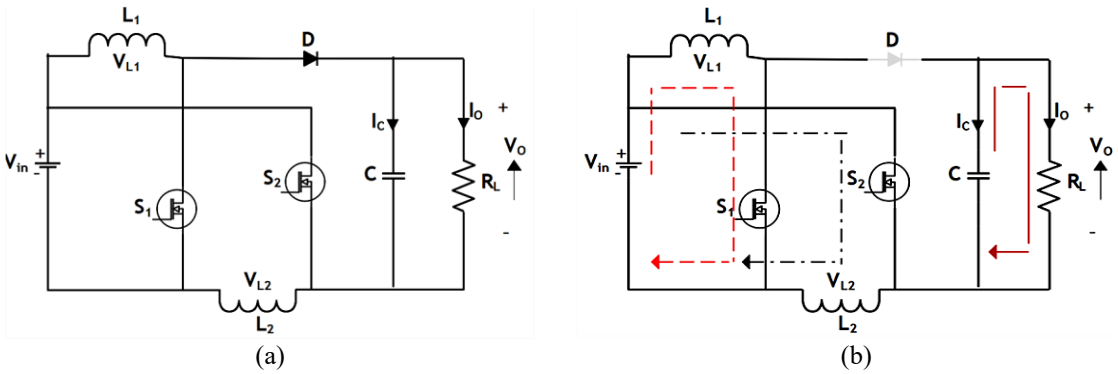

Figure 1. Modified boost converter: (a) circuit diagram and (b) mode 1 circuit

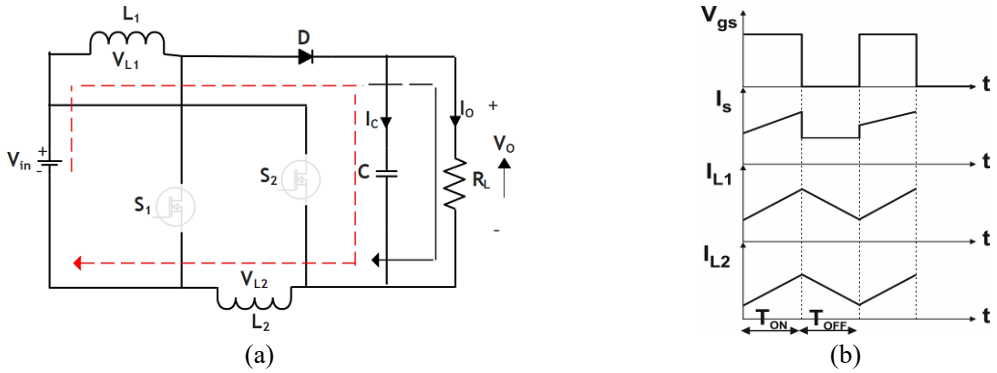

Figure 2. Modified boost converter: (a) mode 2 circuit and (b) V and I waveforms

3. DESIGN PROCEDURE

By applying the volt-second balancing principle, the static gain of the MBC is derived. This derivation uses the relationships expressed in (2) and (9), as shown in (15) and (16).

$$\int_0^{dT} \frac{di_{L1}}{dt}\, dt + \int_{dT}^{(1-d)T} \frac{di_{L1}}{dt} dt = 0 \tag{15}$$

$$\int_0^{dT} \frac{V_{in}}{L_1} dt + \int_{dT}^{(1-d)T} \frac{V_{in}-v_c}{2L_1} = 0 \tag{16}$$

On simplifying (16), the voltage conversion gain of the MBC is:

$$\frac{V_0}{V_{in}} = \frac{1+d}{1-d} \tag{17}$$

3.1. Inductor selection

Source voltage, ripple current, operating frequency, and duty ratio are some of the variables that affect the choice of inductors L_1 and L_2. The (18)–(20) provide the inductance value needed for the high-gain modified converter to function in continuous conduction mode.

$$V_L = L\frac{di}{dt} = V_{in} \tag{18}$$

$$V_L = L\frac{\Delta i}{\Delta t} = V_{in} \tag{19}$$

The inductor ripple is calculated as:

$$L_1 = L_2 = \frac{V_{in}D}{\Delta i_L f_s} \tag{20}$$

3.2. Capacitor selection

The filter capacitor value of the converter is computed using output power rating (P), output voltage, voltage ripple of the capacitor, and frequency. The calculation is presented in (21).

$$C = \frac{P}{V_0 \Delta v_c f_s} \tag{21}$$

3.3. Voltage stress on power switch and diode

The potential stress V_{DS1} and V_{DS2} on power switches S_1 and S_2 is evaluated. The analytical expression is presented in (22).

$$V_{DS1} = V_{DS2} = \frac{V_{in}+V_0}{2} \tag{22}$$

The voltage across the diode VD is given in (23).

$$V_D = V_{in} + V_o \tag{23}$$

4. DYNAMIC ANALYSIS AND DESIGN OF CONTROLLER FOR MBC

The behavior of a power converter over a time can be articulated by its generalized state space average model. This is presented in equations (24) and (25).

$$\frac{dx(t)}{dt} = Ax(t) + Bu(t) \tag{24}$$

$$y(t) = Cx(t) + Du(t) \tag{25}$$

Where A=$A_1 d + A_2(1-d)$, $B = B_1 d + B_2(1-d)$,$C = C_1 d + C_2(1-d)$, $D = D_1 d + D_2(1-d)$, and d is duty cycle. From (5), (6), (13), and (14), the state space expression of the MBC is given in (26) and (27).

$$\begin{pmatrix} \frac{di_{L1}}{dt} \\ \frac{di_{L2}}{dt} \\ \frac{dv_c}{dt} \end{pmatrix} = \begin{pmatrix} 0 & 0 & \frac{-(1-d)}{2L_1} \\ 0 & 0 & \frac{-(1-d)}{2L_2} \\ \frac{1-d}{C} & 0 & \frac{-1}{R_L C} \end{pmatrix} \begin{pmatrix} i_{L1} \\ i_{L2} \\ v_c \end{pmatrix} + \begin{pmatrix} \frac{1+d}{2L_1} \\ \frac{1+d}{2L_2} \\ 0 \end{pmatrix} (V_{in}) \tag{26}$$

$$V_0 = (0 \quad 0 \quad 1) \begin{pmatrix} i_{L1} \\ i_{L2} \\ v_c \end{pmatrix} \tag{27}$$

The open loop transfer equation of the modified boost converter with specification in Table 1 yields in (28).

$$TF = \frac{v_0}{v_{in}} = \frac{2.269e^5 s}{s(s^2+5.739s+4.95e^4)} \tag{28}$$

The previously stated transfer equation is deduced to be a second-order system from (28). Figure 3 displays the frequency characteristics under open loop conditions. The open-loop system exhibits a phase margin of 0.762 degrees, with complex conjugate poles positioned at (-2.87 - j222) and (2.87 + j222) within the negative real axis. To improve the transient response and increase the phase margin, a lead compensator is designed. The generalized transfer function of the lead compensator is given in (29).

$$G_c(s) = \alpha\left(\frac{1+sT}{1+s\alpha T}\right) \tag{29}$$

The closed loop control of MBC is shown in Figure 4. The error signal computed from V_{ref} and V_{mea} is given as input to the lead compensator $G_c(s)$. The output of the compensator e_c is fed to the plant transfer equation G(s). The output of the plant function G(s) is multiplied with feedback H(s) to get the V_{mea} signal. The value of feedback H(s) is considered as unity. The overall transfer expression in closed loop is given in (30).

$$TF = \frac{v_0}{v_{in}} = \frac{1.008e^6 s^2+3.468e^8 s}{s^4+1534s^3+1.067e^6 s^2+4.225e^8 s} \tag{30}$$

The frequency response of the closed loop system is presented in Figure 5. The stability of the system is evident with an infinite gain margin, and the closed-loop system exhibits a phase margin of 76.8 degrees.

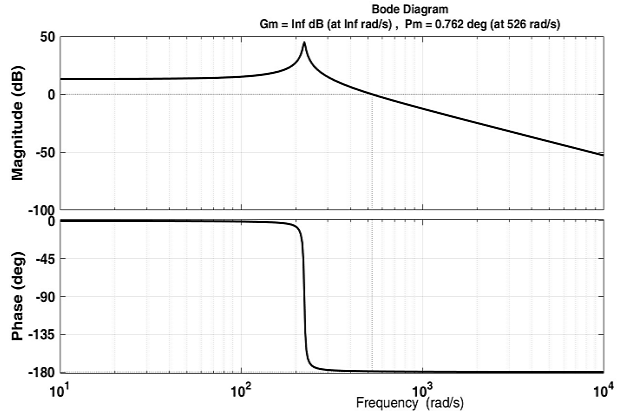

Figure 3. Frequency response under open loop condition

Table 1. Comparative analysis of the MBC with other topologies

Parameters	Boost converter	Ref. [4]	Ref. [5]	Ref. [10]	Modified boost
Voltage gain	1/1-D	(1+D)/(1-D)	1/D(1-D)	(3-2D))/(1-2D	(1+D)/(1-D)
Voltage stress on switch	V_0	-	$(V_{co}-V_{S2})$	$(V_0-V_{in})/2$	$(V_0+V_{in})/2$
Voltage stress on diode	V_0	$V_{c2}-V_{c3}$	-	(V_0-V_{in})	(V_0+V_{in})
Switch count	1	1	2	2	2
Inductors count	1	2	2	1	2
Capacitor count	1	3	2	3	1
Diode count	1	3	3	4	1

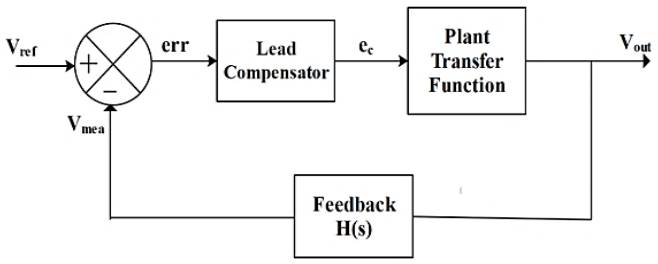

Figure 4. Closed loop control of high gain boost converter

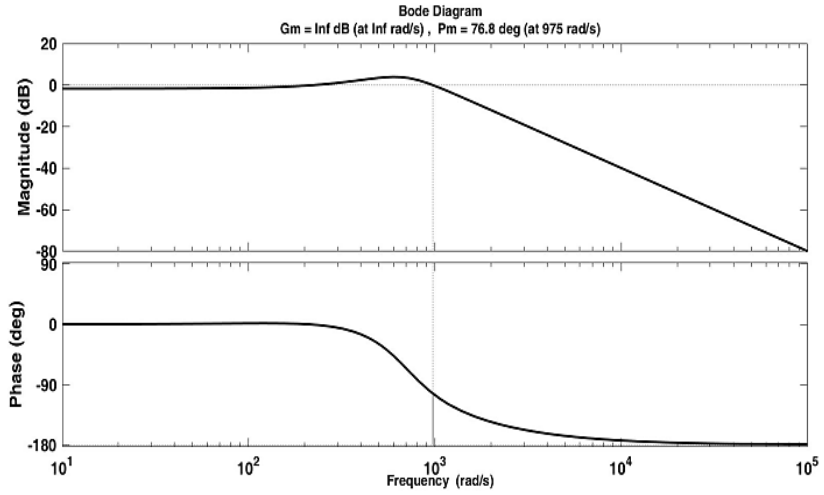

Figure 5. Frequency response under closed loop condition

5. PERFORMANCE COMPARISON

Table 1 displays the comparison of the MBC's performance with that of other converters. A duty ratio comparison of the MBC's static gain with various boost converters is displayed in Figure 6. The MBC delivers the uppermost voltage gain of 19, which is 1.8 times higher than that of a boost converter. The MBC and the converter in [4] have a similar voltage conversion ratio, but the converter in [4] uses a voltage lift technique to augment the static gain. The MBC's voltage conversion ratio is 19.15% elevated than that of the converter topology in [5]. Furthermore, the modified boost converter's output voltage is around 70% more than that of the boost converter when operated at 0.7 duty ratio. While the modified converter necessitates additional inductors and power switches, it achieves parity with the boost structure regarding the quantity of diodes and capacitors employed. In contrast to the converters outlined in references [5] and [10], the proposed boost converter employs fewer circuit elements. The amount of voltage stress on the redesigned converter is estimated to be 60% of the potential at the output. In contrast, the boost converter's power switch voltage loss corresponds to 100% of the load side potential. Hence, the power switch voltage drop is lower in the MBC than in the boost converter. The reduction in switch voltage stress leads to reduce the power loss in switches thereby improving efficiency. The increase in voltage stress leads to reduce lifetime of the switch. However, the converters in [5] and [10] use either switched capacitor or voltage lift method, resulting in lesser voltage drop. The inductors placed in series with the switch stores the energy during ON time and release the energy

during OFF time. Thus improves the voltage of the output. The efficacy of MBC at the rated condition is approximately 94.6%. The MBC can use the onboard charging unit in E-vehicles. Increase in output voltage to a large extent, leads to reverse recovery problem is the limitation of MBC. The modifications in the MBC for fast charging are replacing silicon devices with wide band gap devices; replace diodes by means of bidirectional switches enables bidirectional power flow in the MBC. This modification leads to high cost but improves the performance.

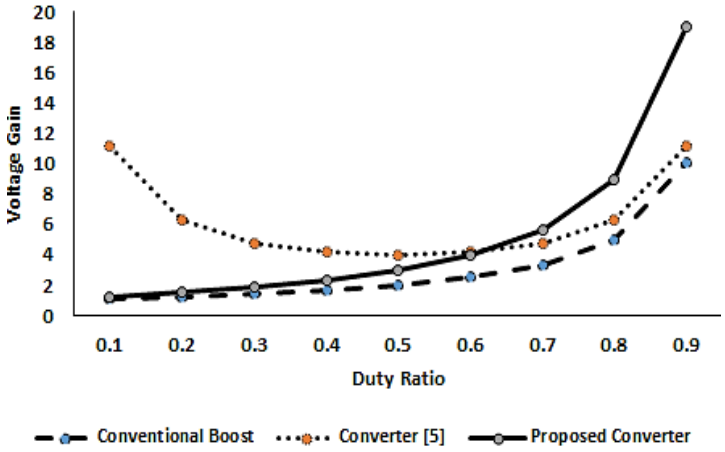

Figure 6. Voltage gain comparison

6. RESULTS AND DISCUSSION

The MATLAB Simulink tool is used to develop and simulate the MBC. The modified converter is specified for 100 W power, operating with a source voltage of 48 V. The planned structure maintains a potential at the load side to 200 V_{dc}. The resistive load is considered for simulation and experimental analysis with circuit parameters tabulated in Table 2. The theoretical idea of the MBC operating in continuous conduction mode (CCM) is validated by the development of a virtual and experimental laboratory model.

The Simulink diagram and the corresponding diode and inductor voltage and current waveforms are shown in Figures 7(a)-7(c) (see Appendix). The prototype, depicted in Figure 7(d) (see Appendix) and its corresponding experimental results are shown in Figures 7(e)-7(g) (see Appendix). Gating pulses were generated by a PIC 18F452 microcontroller, utilizing its CCP unit to achieve a specified operating frequency of 21 kHz. With a source input of 48 V, the prototype achieved a voltage gain of 9.53, resulting in an output voltage of 200 V, as illustrated in Figure 7(e). These experimental findings align closely with the simulated and theoretical values, validating the efficacy of the proposed boost topology design. Figures 7(f) and 7(g) depict the waveforms of inductor and diode's current and voltage, respectively. Analysis of these waveforms revealed an average source current of 1.36 A for a load power of 100 W, with an average load current of 490 mA under the same load power. Notably, the voltage across the diode was observed to be the addition of the voltages at the input and output, corroborating the theoretical calculations. Furthermore, the mean voltage stress across the switch was approximately 58 V, indicating that the potential across the switches S_1 and S_2 averaged the input and output voltages. This observation underscores the efficiency of the MBC in minimizing voltage drop across the switches while providing high gain. The experimental efficacy of the MBC was found to be 94.6% under rated load conditions. This high efficiency further validates the practical viability of the MBC design.

Table 2. Simulation specification

Parameters	Value
Supply voltage	48 V
Inductor	0.36 mH
Output capacitor	100 µF
Output voltage	200 V
Switching frequency	21 kHz
Output power	100 W
Power switch	IRFP460
Power diode	MUR3020PT

7. CONCLUSION

The MBC is designed to minimize voltage loss on switches and increase static voltage gain. To increase voltage, this is accomplished by connecting an inductor in series with a switch. This component operates in parallel with a source once the switches are closed and in series with the source once the switches are on. Reliability and efficacy make this topology an excellent option for direct current (DC) microgrid network applications, also, with an output voltage of 200 V_{dc} and a voltage gain 1.8 times higher than a boost converter. It also reduces voltage stress. A 100 W experimental hardware prototype model was used to test the suggested converter, confirming its efficacy.

ACKNOWLEDGMENTS

The authors thank their institution for their extended support throughout this work.

FUNDING INFORMATION

The authors state there is no funding involved.

AUTHOR CONTRIBUTIONS STATEMENT

This journal uses the Contributor Roles Taxonomy (CRediT) to recognize individual author contributions, reduce authorship disputes, and facilitate collaboration.

Name of Author	C	M	So	Va	Fo	I	R	D	O	E	Vi	Su	P	Fu
Jayanthi Kathiresan	✓	✓	✓	✓	✓	✓		✓	✓	✓				
Gnanavadivel Jothimani		✓			✓	✓	✓	✓		✓	✓	✓		

C : **C**onceptualization
M : **M**ethodology
So : **So**ftware
Va : **Va**lidation
Fo : **Fo**rmal analysis
I : **I**nvestigation
R : **R**esources
D : **D**ata Curation
O : Writing -**O**riginal Draft
E : Writing - Review &**E**diting
Vi : **Vi**sualization
Su : **Su**pervision
P : **P**roject administration
Fu : **Fu**nding acquisition

CONFLICT OF INTEREST STATEMENT

Authors state no conflict of interest.

INFORMED CONSENT

We have obtained informed consent from all individuals included in this study.

DATA AVAILABILITY

Data availability is not applicable to this paper.

REFERENCES

[1] W. Li, Y. Zhao, Y. Deng, and X. He, "Interleaved converter with voltage multiplier cell for high step-up and high-efficiency conversion," *IEEE Transactions on Power Electronics*, vol. 25, no. 9, pp. 2397–2408, 2010, doi: 10.1109/TPEL.2010.2048340.

[2] M. Forouzesh, Y. P. Siwakoti, S. A. Gorji, F. Blaabjerg, and B. Lehman, "Step-up DC--DC converters: a comprehensive review of voltage-boosting techniques, topologies, and applications," *IEEE Transactions on Power Electronics*, vol. 32, no. 12, pp. 9143–9178, 2017, doi: 10.1109/TPEL.2017.2652318.

[3] F. M. Shahir, E. Babaei, and M. Farsadi, "Voltage-lift technique based non-isolated boost DC--DC converter: analysis and design," *IEEE Transactions on Power Electronics*, vol. 33, no. 7, pp. 5917–5926, 2018, doi: 10.1109/TPEL.2017.2740843.

[4] F. M. Shahir, E. Babaei, and M. Farsadi, "Extended topology for a boost DC--DC converter," *IEEE Transactions on Power Electronics*, vol. 34, no. 3, pp. 2375–2384, 2019, doi: 10.1109/TPEL.2018.2840683.

[5] J. Ahmad, M. D. Siddique, A. Sarwar, and C. H. Lin, "A high gain non-inverting DC--DC converter with low voltage stress for industrial applications," *International Journal of Circuit Theory and Applications*, vol. 49, pp. 4212–4230, 2021, doi: 10.1002/cta.3129.

[6] J. Zhao and D. Chen, "Switched-capacitor high voltage gain Z-source converter with common ground and reduced passive component," *IEEE Access*, vol. 9, pp. 21395–21407, 2021, doi: 10.1109/ACCESS.2021.3054880.

[7] K. Jayanthi, N. S. Kumar, and J. Gnanavadivel, "Design and implementation of modified SEPIC high gain DC--DC converter for DC microgrid applications," *International Transactions on Electrical Energy Systems*, vol. 31, 2021, doi: 10.1002/2050-7038.12921.

[8] K. Jayanthi and J. Gnanavadivel, "High gain converter design and implementation for electric vehicles," *International Journal of Electrical and Electronics Research*, vol. 10, no. 4, pp. 1058–1063, 2022, doi: 10.37391/IJEER.100449.

[9] J. Gnanavadivel, K. Jayanthi, S. Vasundhara, K. V Swetha, and K. J. Keerthana, "Analysis and design of high gain DC--DC converter for renewable energy applications," *Automatika*, vol. 64, no. 3, pp. 408–421, 2023, doi: 10.1080/00051144.2023.2170062.

[10] A. Samadian, S. H. Hosseini, M. Sabahi, and M. Maalandish, "A new coupled inductor non-isolated high step-up quasi Z-source DC--DC converter," *IEEE Transactions on Industrial Electronics*, vol. 67, no. 7, pp. 5389–5397, 2020, doi: 10.1109/TIE.2019.2934067.
[11] M. K. Rathi, J. Gnanavadivel, and K. Jayanthi, "Augmented ASC network for photo voltaic applications," *International Journal of Electrical and Electronics Research*, vol. 10, no. 3, pp. 544–549, 2023, doi: 10.37391/IJEER.100323.
[12] M. Zamani, A. Aghaie, A. Zamani, R. Tari, M. Abarzadeh, and S. H. Hosseini, "Design and implementation of non isolated high step-up DC-DC converter," *International Transactions on Electrical Energy Systems*, p. 4016996, 2023, doi: 10.1155/2023/4016996.
[13] V. Saravanan, M. Sabitha, V. Bindu, K. M. Venkatachalam, and M. Arumugam, "Single switch Z-source/quasi Z-source DC--DC converters," *International Journal of Applied Power Engineering*, vol. 10, no. 1, pp. 68–79, 2022, doi: 10.11591/ijape.v10.i1.pp68-79.
[14] M. V. G. Varaprasad *et al.*, "Design and analysis of PV fed high-voltage gain DC--DC converter using PI and NN controllers," *Ain Shams Engineering Journal*, vol. 14, no. 8, 2023, doi: 10.1016/j.asej.2022.102061.
[15] J. P. Phatak, L. Venkatesha, and C. S. Raviprasad, "Driving cycle based battery rating selection and range analysis in EV applications," *International Journal of Power Electronics and Drive Systems*, vol. 12, no. 2, pp. 637–649, doi: 10.11591/ijpeds.v12.i2.pp637-649.
[16] W. Hassan, J. L. Soon, D. D. C. Lu, and W. Xiao, "A high conversion ratio and high-efficiency bidirectional DC--DC converter with reduced voltage stress," *IEEE Transactions on Power Electronics*, vol. 35, no. 11, pp. 11827–11842, 2020, doi: 10.1109/TPEL.2020.2987083.
[17] J. Liu, J. Wu, J. Qiu, and J. Zeng, "Switched Z-source/quasi-Z-source DC--DC converters with reduced passive components for photovoltaic systems," *IEEE Access*, vol. 7, pp. 40893–40903, 2019, doi: 10.1109/ACCESS.2019.2907300.
[18] M. Veerachary and P. Sen, "Dual-switch enhanced gain boost DC--DC converters," *IEEE Transactions on Industry Applications*, vol. 58, no. 4, pp. 4903–4913, 2022.
[19] C.-W. Ding and P.-C. Tung, "A new approach to field-oriented control that substantially improves the efficiency of an induction motor with speed control," *Applied Sciences*, vol. 15, no. 9, 2025, doi: 10.3390/app15094845.
[20] K. Zhou, H. Yang, Y. Zhang, Y. Che, Y. Huang, and X. Li, "A review of the latest research on the topological structure and control strategies of on-board charging systems for electric vehicles," *Journal of Energy Storage*, vol. 97, p. 112820, 2024, doi: 10.1016/j.est.2024.112820.
[21] D. Pesantez, O. Menendez, H. Renaudineau, S. Kouro, S. Rivera, and J. Rodriguez, "Intelligent control for Type I partial power converters in EV charging systems: twin-delayed deep deterministic policy gradient approach," in *2024 IEEE International Conference on Automation/XXVI Congress of the Chilean Association of Automatic Control (ICA-ACCA)*, 2024, pp. 1–6, doi: 10.1109/ICA-ACCA62622.2024.10766834.
[22] K. Zhou, Y. Wu, X. Wu, Y. Sun, D. Teng, and Y. Liu, "Research and development review of power converter topologies and control technology for electric vehicle fast-charging systems," *Electronics*, vol. 12, no. 7, p. 1581, 2023, doi: 10.3390/electronics12071581.
[23] A. B. Reddy, S. N. Mahato, and N. Tewari, "Dual switch ultra-high gain DC--DC converter with low voltage stress," *AEU - International Journal of Electronics and Communications*, vol. 173, 2024, doi: 10.1016/j.aeue.2023.154995.
[24] S. D. Gangula, T. K. Nizami, and R. R. Udumula, "Self-learning controller design for DC--DC power converters with enhanced dynamic performance," *Journal of Control, Automation and Electrical Systems*, vol. 35, pp. 532–547, 2024, doi: 10.1007/s40313-024-01086.
[25] P. Vishnuram *et al.*, "A comprehensive review on EV power converter topologies, charger types, infrastructure and communication techniques," *Frontiers in Energy Research*, vol. 11, 2023, doi: 10.3389/fenrg.2023.1103093.

APPENDIX

(a)

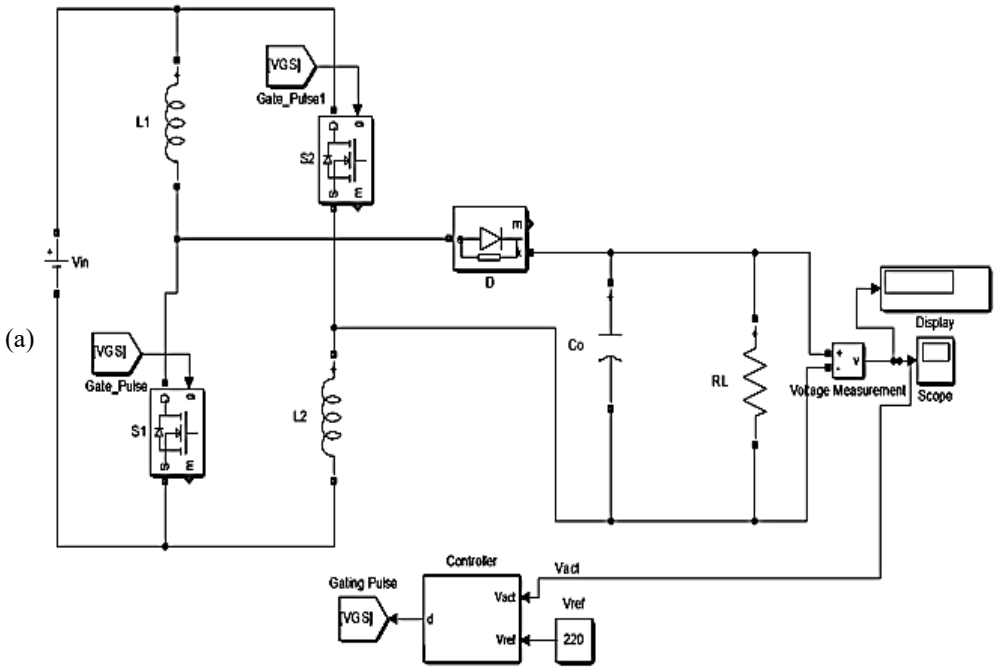

Figure 7. Hardware waveforms: (a) Simulink diagram of MBC

(b)

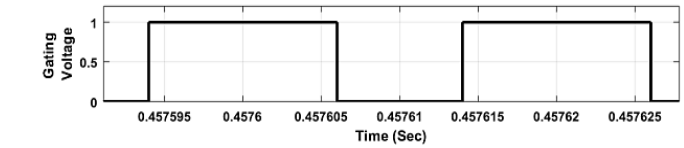

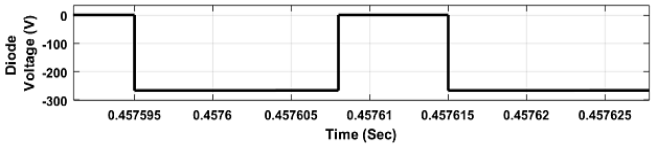

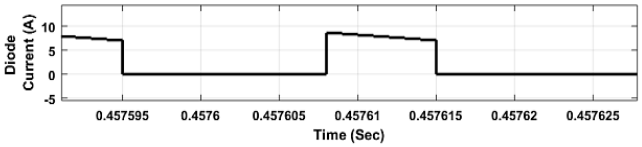

(c)

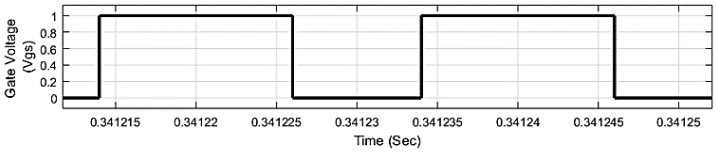

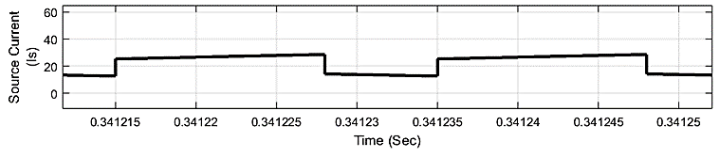

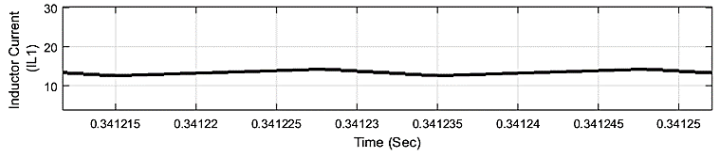

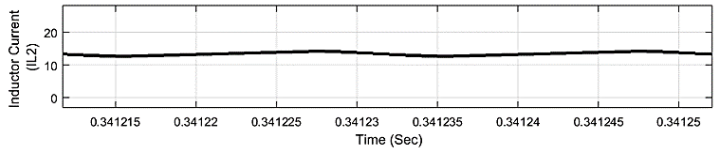

(d)

(e)

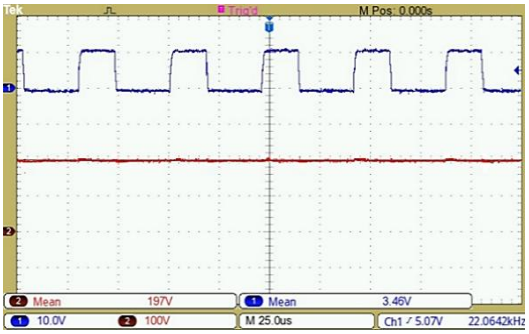

Figure 7. Hardware waveforms: (b) simulated diode voltage waveform, (c) simulated inductor current waveform, (d) prototype model, and (e) output voltage (continued)

(f)

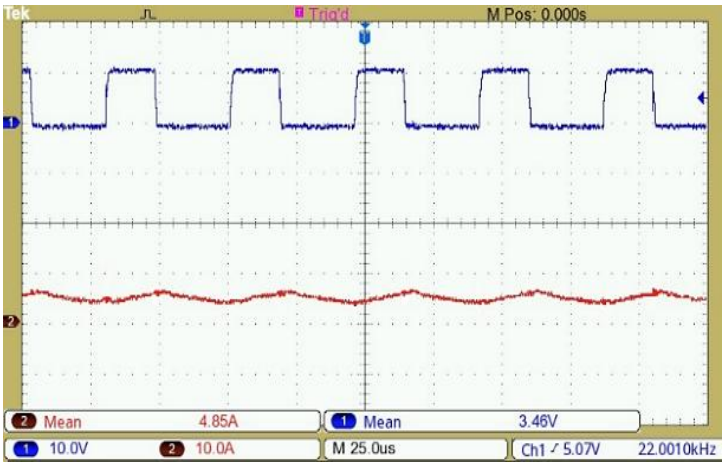

(g)

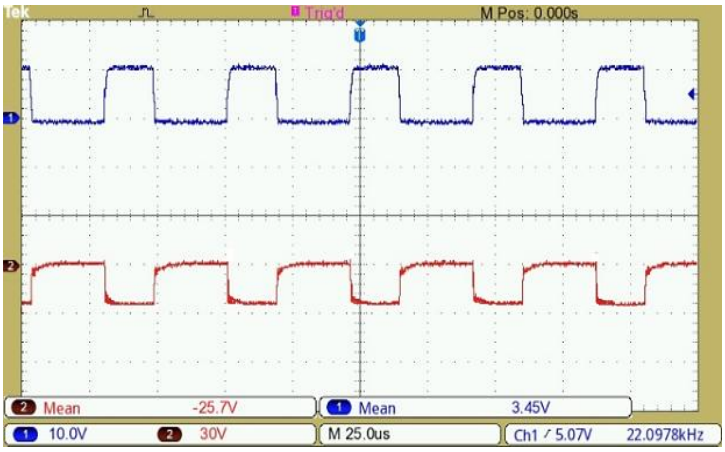

Figure 7. Hardware waveforms: (f) inductor current (I_{L1}, I_{L2}) and (g) diode voltage (D_0) (continued)

BIOGRAPHIES OF AUTHORS

Dr. Jayanthi Kathiresan received her B.E. in Electrical and Electronics Engineering from Madurai Kamaraj University, Madurai. She received her M.E. in Applied Electronics and Ph.D. in Electrical Engineering from Anna University, Chennai. At present, she is working as an Associate Professor in the Department of Electrical and Electronics Engineering, Mepco Schlenk Engineering College, Sivakasi. She can be contacted at email: kjayanthi@mepcoeng.ac.in.

Dr. Gnanavadivel Jothimani received his B.E. in Electrical and Electronics Engineering from Madras University, Chennai. He received his M.E. in Power Electronics and Drives from Bharathidasan University. He received his Ph.D. in Power Quality in Power Converters from Anna University, Chennai. At present, he is working as an Associate Professor in the Department of Electrical and Electronics Engineering, Mepco Schlenk Engineering College, Sivakasi. He can be contacted at email: gvadivel@mepcoeng.ac.in.